Analyzing the Force Variation and Response of a Human Body Finite Element Model in the Underbody Blast Environment

Zachary S. Hostetler, Jazmine Aira, Juliette Caffrey, F. Scott Gayzik

Abstract

The objective of this work was to use the Global Human Body Models Consortium (GHBMC) model to analyze force variation as a function of underbody blast (UBB) loading severity and to assess the suitability of this human model for use in this environment. A design of experiments (DOE) was conducted across a wide range of input pulses representing UBB loading conditions. 51 whole body simulations were conducted (peak velocity range 2-15 m/s and time to peak 2-20 ms). The GHBMC M50-O (v 5.0) was positioned in the finite element (FE) setup, booted, and belted with a five point harness. Time history of force data were extracted from the lower extremity (calcaneus, tibia, femur), pelvis (superior and inferior pubic rami), and the spine (L5, L3, T12, T6, T1, C1). Out of the 51 simulations that were conducted (94%) yielded actionable (the last time step beyond peak load values at all areas of interest) data. The greatest force values and ranges were observed in the thoracic and lumbar spine: T12 (5.30±1.90 kN), L3 (5.39±1.91 kN), and L5 (5.83±2.06 kN). The lowest force values were observed in the femur (0.71±0.32 kN). C1 (2.5±0.53 kN) experienced more loading compared to T1 (1.07±0.23 kN). Time to peak velocity did not have a significant effect on the force response. Furthermore, the force values observed are within ranges of previously reported values. The data indicate that the model may be suitable for use in the UBB environment.

Keywords (5) Finite-element, GHBMC, human body model, lower extremity, under-body blast

I. INTRODUCTION

Increased modernization and technological advances have drastically changed modern warfare. In Operation Iraq Freedom (OIF) and Operation Enduring Freedom (OEF), improvised explosive devices (IEDs) were the single most prevalent threat to soldiers, accounting for 45.6% of all combat deaths [1] and were the leading cause of vehicle loss [2]. It is also important to note that IED explosions have occurred outside of warzone areas. In 2012, there were an average of 500 IED explosions per month worldwide (excluding Iraq and Afghanistan) [3]. IEDs pose a serious threat to soldiers in vehicles as the explosion causes a high amount of energy to be transferred from the floor of the vehicle directly to the lower extremities and from the seat of the vehicle directly to the pelvis. In a recent case review of injuries in OIF and OEF directly related to underbody blasts (UBBs), Danelson et al. found that lower extremity injuries were the most frequent. Seventy-nine percent of the injuries reviewed were AIS2+ fractures with the distal tibia, distal fibula, and calcaneus being the most commonly fractured bones. While lower extremity injuries were the most common, the most severe injuries occurred in the pelvis, lumbar spine, and thoracic spine [4]. There is a clear need to develop testing protocols and better understand the injury mechanism in the UBB environment for soldier protection. The loading direction and UBB pulse characteristics are just two of the many distinct characteristics that make the UBB environment difficult to study and replicate physical testing. IED's can be located at the side, front, or rear of the vehicle and have a non-vertical main loading direction Furthermore, IEDs on the roof of the vehicle can create even greater challenges. The blast pulse from an IED has a peak acceleration 5-10 times greater and the duration of the pulse is 3-5 times shorter [5]. Ramasay et al. reported UBB floor plates can reach up to 30 m/s in 6-10 ms [6] and Bird et. al reported floor pan accelerations in excess of 100 G's in 3-100 ms [7].

Experimental work in the UBB environment has been conducted with both anthropomorphic test devices (ATDs) and postmortem human subjects (PMHS). Danelson et al. [8] used an Accelerative Loading Fixture (ALF)

Z.S. Hostetler and J. Caffrey are PhD students in Biomedical Engineering. J. Aira is a research engineer in the Dept. of Biomedical Engineering and F. Scott Gayzik (sgayzik@wakehealth.edu, +1 336-716-6643) is an Associate Professor of Biomedical Engineering Wake Forest School of Medicine, USA.

to study UBB events in a more controlled laboratory setting. Fourteen tests were conducted using both PMHS and the Hybrid-III ATD. The results showed that the Hybrid-III ATD was not able to be positioned in accordance with the PMHS in the rigid seat and exhibited a stiffer overall response. Furthermore, the ATD was not able to capture the kinematic response of the PMHS lower extremities. To overcome the shortcomings of the Hybrid-III in the vertical loading environment, the U.S. Army began the Warrior Injury Assessment Manikin (WIAMan) project and development of the WIAMan ATD. The WIAMan ATD response was compared to matched pair testing of Post-Mortem Human Subject (PMHS) in a variety of sub-injurious loading conditions. The testing conditions were designed to mimic loading conditions of a seated soldier with and without Personal Protective Equipment (PPE). The model response was compared to the PMHS response and quantitatively evaluated using corridor methods outlined in [9]. Overall, the ATD achieved biofidelity score ranges between 0.59 - 0.63 for the three different test conditions, indicated a fair ATD response based on CORA guidelines and ratings compared to the PMHS test subjects [10].

PMHS testing has been conducted both at a component level and whole body level, focusing on lower extremity and more recently pelvis and lumbar spine injuries. Chirvi et al. used a compilation of lower extremity data from pendulum impacts [11,12] as well as vertical loading [12,13] to develop injury risk curves from PMHS data[14]. Despite a larger sample size from a combination of studies and varying the posture and footwear (booted vs non-booted), posture was not a significant covariate in the final injury risk model. Footwear was initially a significant covariate but was removed as the fracture tolerance of a bone should be independent of the presence of footwear [13]. It was noted that the presence of a boot shifted the injury pattern to tibia injuries whereas the unbooted specimens experienced primarily calcaneus injuries. This trend was further confirmed and supported by the work of Hampton et al. by analyzing the force mitigation the boot provides [15]. The work done by Bailey et al. examined the whole body response of 10 PMHS subjects using the ODYSSEY blast rig. The seat pan accelerations ranged from 291-738 G's and the floor plan accelerations ranged from 234-858 G's over the course of 3 ms. The outcome of the work focused on injury threshold values specifically in the lower extremity and pelvic regions. The lower extremity fractures observed were consistent with previously reported literature about high rate axial loading and UBB events [16,17]. The pelvic injuries noted were similar to what has been reported in the UBB environment but an important finding was the loading rate with respect to the injury location[18,19]. The authors proposed that the high rate loading events produced injuries closer to the loading area whereas the lower loading rates produced injuries further away from the loading area [20]. Dooley et al. carried out whole body PMHS experiments using the Vertically Accelerated Load Transfer System (VALTS) at the Johns Hopkins Applied Physics Laboratory (APL). Seven specimens were tested in UBB conditions (lower extremity peak velocity varied from 4-8 m/s and pelvis peak velocity varied from 4-6 m/s with a time to peak (TTP) all between 5-10 ms). The study showed that load severity, bone quality and spinal alignment all showed influence on vertebral compression fracture but no single factor was able to distinguish injury criteria by itself.

Human body models (HBMs) have been developed and are used to study injury risk through computational simulations and FE analysis. The Global Human Body Models Consortium (GHBMC) M50-O average male seated occupant is a widely used and validated HBM [21,22]. On a component level, the PLEX (pelvis and lower extremity) have been validated in numerous loading conditions including axial loading. The ankle has been specifically studied in impacts for axial loading, ankle inversion, eversion, dorsiflexion, and rotation [16,23-25]. The tibia has been validated in a three-point bending setup as well as axial loading for the entire leg [26,27]. The pelvis has been validated in quasi-static and dynamic compression as well as in dynamic impacts to the iliac wing and acetabulum [19,28]. These studies aimed primarily at validation and model assessment for the automotive environment but more recently, HBMs have been used to study injury risk in the UBB environment. Gabler et al. investigated the GHBMC response in two UBB loading conditions. The study found that the material properties used for the plantar surface of the foot were highly sensitive to the rate of loading and affected the peak force response of the model [29]. Weaver et al. investigated the pelvic response of the GHBMC and found that the model response was well correlated with peak forces and strains used to develop injury risk curves from PMHS subjects [30].

While the use of HBMs in the UBB environment has increased and shown positive results, the potential of these models has not been fully explored. This is due to models not being widely available and/or develop for specific cases (e.g. Hampton et al. [15]) or prohibition of use in the military environment. Finally, an advantage of HBMs is the large scale testing and design of experiments (DOE) studies that can be conducted to improve model response and develop model specific injury risk curves to aid in soldier protection and safety. This large scale testing is not feasible for physical experiments due to the cost and destructive nature of the test environment. Therefore, the objective of this study is to use the GHBMC M50-O model to analyze force variation as a function of the UBB loading severity. Model analysis will focus on the lower extremity, pelvis and spine due to commonality and severity of the injuries experienced in modern warfare.

II. METHODS

Design of Experiments Sample Space

A design of experiments (DOE) was conducted to analyze force variation in the body across a range of input pulses representing UBB loading conditions. The input sample space was developed from previous studies [5,8,20] and with the use of a computational approach, was extended beyond the STANAG 4569 [31] injury tolerance range of 5 m/s to test model stability. Fifty-one whole body simulations were conducted with a peak seat velocity range of 2-15 m/s and time-to-peak of 2-20 milliseconds (Figure 1).

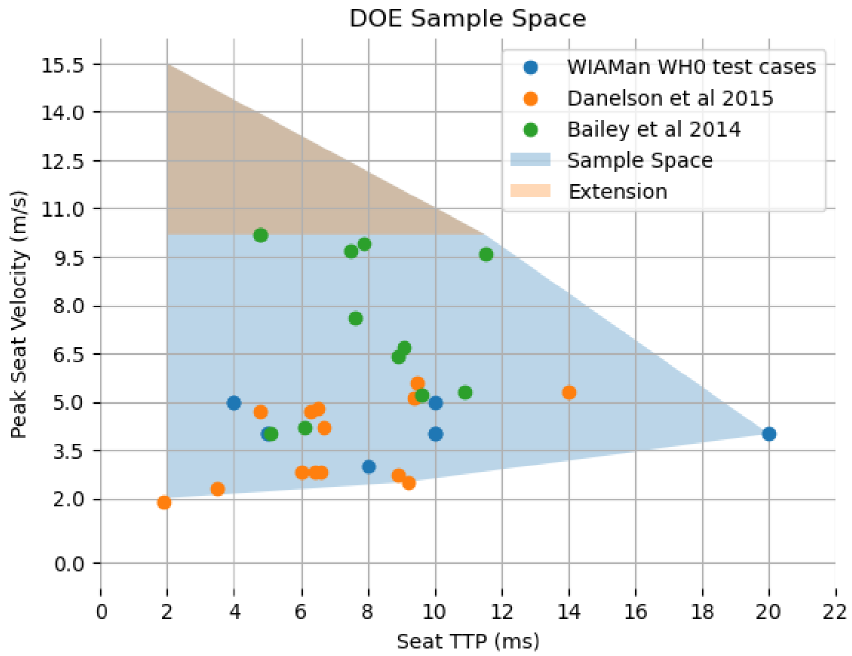

Figure 1. Design of Experiments (DOE) sample space for seat time to peak and peak velocity. The blue region indicates previously reported values and the red region is the extension of the space to test model stability in high rate loading conditions.

The input pulses were applied to the model as a velocity-time history trace in LS-DYNA using the *Boundary_prescibed_motion card. The inputs were based off reported values in Ott et al. [32] and three different pulse characteristics were considered: seat TTP velocity, seat peak velocity, and seat pulse duration. From these three characteristics a simplified, triangular velocity curve was developed (a linear increase to the specified time-to-peak, and then a linear decrease back to v = 0 m/s) and used to generate 51 unique loading curves. The relationship for each characteristic (TTP, peak, and duration) between the seat and floor from the reported values were used to develop scaling relationships between the seat and floor pulses. A unique trace was applied to both the seat and the floor for each simulation.

Human Body Model Boot Donning and Model Positioning

The GHBMC M50-O (v 5.0) was fit with a boot model provided by the sponsor (U.S. Army Research Laboratory). The boot has been previously validated in ATD studies [33]. The fitting was accomplished by artificially decreasing the size of the foot to fit within the native boot and then allowing the human foot model to linearly increase to its nominal size. The process achieved a smooth fit between the human model's leg and foot and the surrounding boot. This was conducted first to allow for any natural deformations and movement as the model was positioned and belted into the test rig.

The FE setup is based on literature data and is described in greater detail in Ott et al. [32] Briefly, the FE setup consists of a vertical sled system with a rigid seat and aluminum floor plate (Figure 2). The GHBMC M50-O (v 5.0) was positioned in the finite element (FE) setup using published descriptions of post-mortem human subjects (PMHS) to guide positioning [32]. Angle and relative displacement measurements in the head (Frankfurt plane to acromion vertical difference 0.0 ± 20 mm), arms (shoulder-elbow-wrist angle 45-45 deg angle), pelvis (hip-knee-ankle angle 90-90-90 deg, and pelvis angle = 40 ± 5 deg) and foot (boot to heel separation 295 mm ± 10 mmposition on floor plate) were taken pre and post positioning and compared to PMHS reported values. Positioning simulations were executed in LS-DYNA using *Boundary_prescribed_final_geometry cards and gravity fields to allow the model to naturally move to the desired positions with correct angle measurements. All angle measurements for the PLEX region were within 5% of reported values and deemed acceptable given the focus on the PLEX region. Furthermore, the model was belted with a five point harness and before each simulation, belts were tightened to 10 lbf. For each of the 51 simulations conducted, the model was allowed 100 milliseconds of gravity settling before each 150 millisecond input pulse was applied to the model.

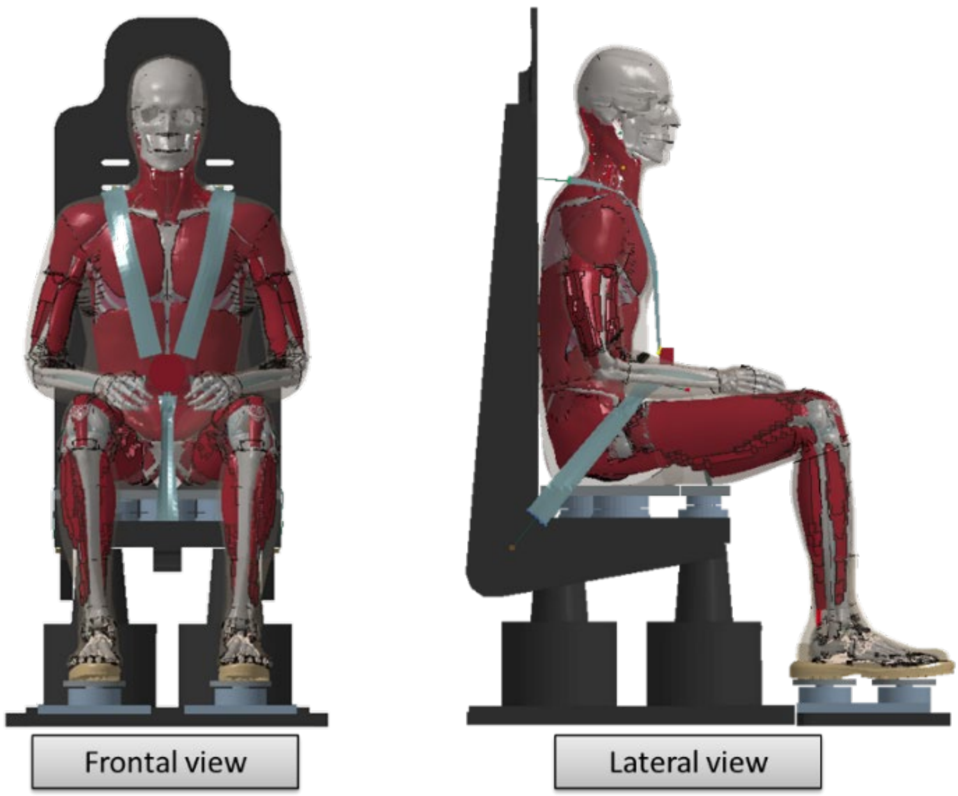

Figure 2. Model positioning showing the frontal view (left) and the lateral view (right) in a 90-90-90 posture for testing with the 5 point harness and military boot.

Human Body Model Instrumentation and Data Reduction

For all simulations conducted in the DOE, fracture status (element deletion based on failure strain criteria) was turned off. Time history for forces and accelerations were extracted from the lower extremities (calcaneus, tibia, femur), pelvis (superior and inferior pubic rami), and the spine (L5, L3, T12, T6, T1, C1). A detailed figure of model cross-sections for data output and coordinate systems are shown in Figure 3. For comparison to published values in the literature, all coordinate systems were implemented using the body centric SAE J211 coordinate system (1995) [34]. All accelerations reported were filtered using a CFC of 1000 and all forces were filtered using a CFC of 600. Furthermore, displacements from a bone were reported as the displacement of an interpolated node at the center of gravity of the bone of interest. Planes for reported forces were instrumented to be normal to the direction of loading and based on their respective SAE J211 coordinate system. To assess the model stability in the UBB environment, post-processing steps included: simulation status upon completion (either normal or error), visual inspection of animation states for any non-physical behavior, and added mass to the model due to mass scaling being less than 1%.

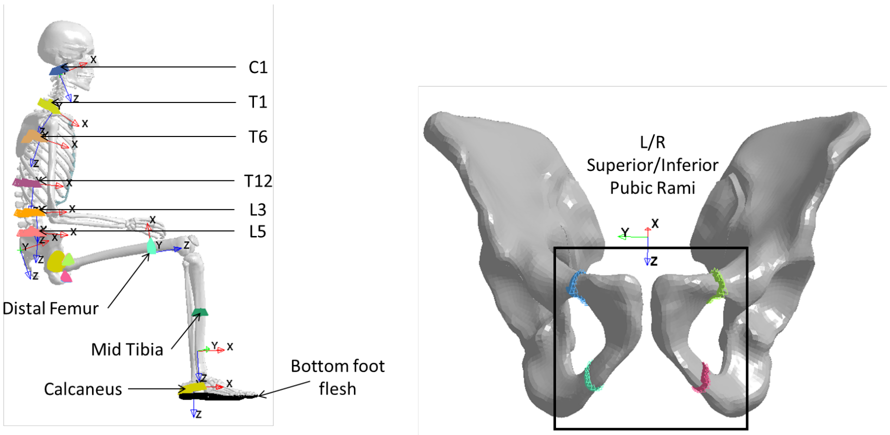

Figure 3. GHBMC M50-O model instrumentation with cross sections and coordinate systems described

III. RESULTS

Overall Status and Model Stability

Out of the 51 simulations that were conducted, 82% resulted in a normal termination status. Forty-eight out of the 51 (94%) yielded actionable data for analysis (the last time step reported was beyond peak load values at all areas of interest). The remaining three simulations that error terminated did so before peak force values were observed in the spine (Figure 4). The simulations that error terminated did so in the bony and flesh region of the pelvis. If failure strains were enabled, there would have likely been a large amount of element deletion indicating pelvis fracture due to the high loading rate experienced by the pelvis from the seat. Overall the model demonstrated stability in the previously reported range of UBB tests, but showed error terminations at severe loading rates beyond those tested (> 12.5 m/s; TTP=2, 4 ms). Furthermore, for the normal terminations the simulation animations showed normal physical responses and the total added mass was less than 1% indicating overall model stability.

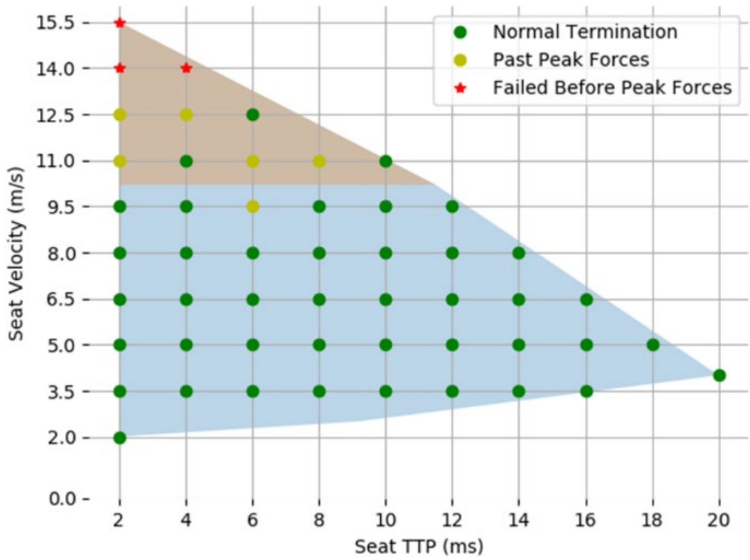

Figure 4. Whole body DOE status for the 51 simulations conducted

Body Region Results

An overview of the peak forces observed in the lower extremities as function of time-to-peak (ms) and peak velocity (m/s) are shown in Figure 5. For all simulations conducted, the forces observed in the femur were lower compared to the forces in the tibia and calcaneus. This is likely due to the use of the SAE J211 coordinate systems and tibia and calcaneus orientation being in the same loading direction compared to the femur. The time to peak force (ms) had less of an influence on the peak force compared to the peak velocity (m/s). Observed forces in the calcaneus and tibia were very similar across all inputs, but the forces in the tibia were slightly higher (2.49 ± 1.38 kN compared to 2.35 ± 1.44 kN).

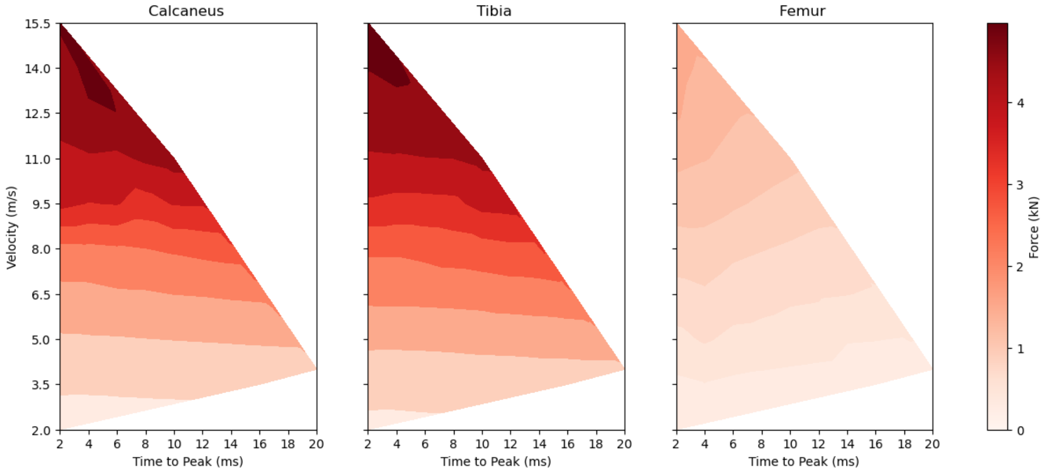

Figure 5. Lower extremity (calcaneus, tibia, and femur) results showing the peak force (kN) response as a function of peak velocity (m/s), time to peak (ms).

In the pelvis, the inferior pubic rami forces were slightly higher compared to the superior pubic rami forces and there was little variation observed between the left and right sides of the pelvis indicating symmetrical loading. Again, the time-to-peak velocity (ms) had a smaller effect on the peak force compared to the peak velocity (m/s). Finally, for forces in the spine, there was a trend of force attenuation moving up the body from L5-T1 with the exception of higher forces observed in C1 compared to T1. The higher forces observed in C1 are likely due to the stiffness and damping observed in the neck and the mass of the head. Furthermore, there were large amounts of neck extension at the C1 level. The greatest forces across all body regions were observed in L5, L3, and T12. For all body regions (lower extremity, pelvis and spine) variation of time-to-peak did not have as great an effect on the peak force as the peak velocity did. This can be seen in the appendix figures Figure A1 A and Figure A1 B. Therefore, for all 51 simulations, the minimum, maximum, and average ± standard deviation force is reported in Table 1 and a boxplot of the force variation across the body regions is shown in the appendix in Figure A1 C.

Table 1. Overview of minimum, maximum, and average ± standard deviation for forces (kN) observed in the different body regions.

Body Region		Min (kN)	Max (kN)	Avg. ± SD (kN)
Lower Extremity	Calcaneus	0.34	4.92	2.35 ± 1.44
	Tibia	0.44	4.97	2.49 ± 1.38
	Femur	0.21	1.53	0.76 ± 0.36
Pelvis	Sup. Pubic Rami	0.22	3.05	1.20 ± 0.71
	Inf. Pubic Rami	0.28	2.80	1.23 ± 0.55
Spine	L5	1.63	9.12	5.83 ± 2.06
	L3	1.48	8.47	5.39 ± 1.91
	T12	1.47	8.67	5.30 ± 1.90
	T6	1.21	5.13	3.57 ± 1.01
	T1	0.47	1.41	1.07 ± 0.23
	C1	1.05	3.04	2.51 ± 0.53

IV. DISCUSSION

PMHS component level testing in the UBB environment has been used to develop biofidelic response corridors [13] and injury risk curves for the leg [14]. However, there has been limited data published for whole body tests. Bailey et al. conducted a study on a similar blast rig (ODYSSEY) and tested 10 PMHS subjects with seat peak velocities ranging from 4.6 to 10.4 (m/s) with a time-to-peak of 4.8 to 9.1 (ms). Floor peak velocities ranged from 4.6 to 10.8 with time-to-peak ranging from 4.1 to 6.7 (ms) [20]. Acceleration data was recorded using accelerometers mounted on the pelvis, distal femur, and distal tibia and pelvis velocity was also calculated. Pelvis acceleration ranged from 100 to 368 (G's) while pelvis velocity ranged from 1.7 to 6 (m/s). The observed pelvis accelerations from the GHBMC M50-O were 23 to 714 G's and the velocities ranged from 1.4 to 9.9 m/s. The PMHS tibia accelerations ranged from 117 to 510 G's and the GHBMC M50-O tibia accelerations ranged from 21.3 to 355.9 G's. While this does not serve as a direct comparison or validation since the test setups were different and used different input traces, the ranges observed by the GHBMC model indicate it is able to capture a wide range of responses and is generally in agreement with PMHS test subjects. The higher values observed in the pelvis are likely due to the extension of the sample space beyond published literature values. The higher forces observed in the tibia compared to the calcaneus are consistent with previously published studies when boot use was present [13,15]. The higher forces observed in the inferior region of the pelvis compared to the superior parts are hypothesized due to the proximity to the seat and high rate loading. Visual inspection of simulation animations showed high amounts of neck extension and could contribute to the higher amounts of forces observed at the C1 level compared to T1. Time-to-peak velocity did not have as great an effect on the peak force as the peak velocity did. This indicates the model may not be as sensitive to the loading rate, but rather the total amount of energy that is imparted into the system.

There are limitations to note about the study. First, the study does not serve as a validation but rather an assessment of the suitability of the GHBMC model for use in this environment. The model is generally stable in all but the most severe loading conditions and appears to provide biomechanical data generally in the range of prior studies. However, since failure was not considered for most long bones, the forces observed will be higher than if element deletion is allowed, but large amounts of element deletion due to failure can lead to model instabilities. Next, further study of the material of some of the points of interaction with its environment may be needed. The lower tibia accelerations observed compared to the Bailey et al. PMHS study [20] could be due to the material model in the GHBMC heel pad. Previous studies have indicated that the heel pad is sensitive to high rate loading and the native material in the model has limitations in this environment [29]. Furthermore, the GHBMC M50-O is "ageless" meaning that while the material definitions and curves used in the model are based on previous component level or whole body tests, the materials come from a wide range of sources and do not represent a younger, active military personnel. PMHS testing is often done on older, male cadavers and therefore the force response could vary with material models based on younger subjects. Additionally, the time-to-peak is extremely short relative to automotive applications and more rate dependent material models may need to be implemented to accurately capture the loading response for these short high rate periods.

V. CONCLUSIONS

The GHBMC M50-O was used to simulate a range of UBB inputs and analyze force variation as a function of velocity in key body regions. C1 experienced higher loads compared to T1 pointing to countermeasures which could be introduced for soldier protection. Overall the model was generally stable and error terminated at severe loading rates (12.5 m/s at 2 ms TTP). Furthermore, the model proved suitable for use in this environment through donning of the military boot, positioning from native, reclined, automotive posture to 90-90-90 seated posture, and belting with the five point harness. Component level tests have been completed using PMHS and ATDs in UBB, whereas the novelty of this study is the use of a human body model in the same environment. The results from this study can be used to compare to physical ATDs designed for the UBB environment, to assess localized injury criteria through element failure or finally used with established PMHS based risk curves to correlate injury risk.

VI. ACKNOWLEDGEMENT

Funding for this work was provided by U.S. Army Med R & D Command, under BAA W911NF-17-S-0003, *Exploring Physics-based Finite Element Analysis of Service Members Subjected to Extreme Environments*. The authors acknowledge the contributions and support of Dr. Michael Kleinberger, Mr. Randolph Coates, and Dr. Kathryn Loftis of the U.S. Army Futures Command. F.S. Gayzik is a member of Elemance, LLC, which provide academic and commercial licenses for GHBMC-owned models.

VII. REFERENCES

[1] Ramasamy, A., Hill, A.M., et al. The modern “deck-slap” injury—calcaneal blast fractures from vehicle explosions. *Journal of Trauma and Acute Care Surgery*, 2011. 71(6): p. 1694-1698

[2] Bird, R. Protection of vehicles against landmines. *Journal of Battlefield Technology*, 2001. 4: p. 14-17

[3] Singleton, J.A., Gibb, I.E., Hunt, N.C., Bull, A.M., and Clasper, J.C. Identifying future ‘unexpected’survivors: a retrospective cohort study of fatal injury patterns in victims of improvised explosive devices. *BMJ open*, 2013. 3(8)

[4] Danelson, K., Watkins, L., et al. Analysis of the Frequency and Mechanism of Injury to Warfighters in the Under-body Blast Environment. 2018, SAE Technical Paper.

[5] Kulkarni, K.B., Ramalingam, J., and Thyagarajan, R. Evaluating the effectiveness of various blast loading descriptors as occupant injury predictors for underbody blast events. 2013, ESI US INC TROY MI.

[6] Ramasamy, A., Hill, A.M., et al. Blast-related fracture patterns: a forensic biomechanical approach. *Journal of the Royal Society Interface*, 2011. 8(58): p. 689-698

[7] Bird, R., Swinton, R., and Krstic, A. Protection of lower limbs against floor impact in army vehicles experiencing landmine explosion. *Journal of battlefield technology*, 2001. 4: p. 8-12

[8] Danelson, K.A., Kemper, A.R., et al. Comparison of ATD to PMHS response in the under-body blast environment. 2015, SAE Technical Paper.

[9] Gayzik, F., Marcus, I., et al. A point-wise normalization method for development of biofidelity response corridors. *Journal of biomechanics*, 2015. 48(15): p. 4173-4177

[10] Pietsch, H.A., Bosch, K.E., et al. Evaluation of WIAMan technology demonstrator biofidelity relative to sub-injurious PMHS response in simulated under-body blast events. 2016, SAE Technical Paper.

[11] Gallenberger, K. Foot and ankle injuries in variable energy impacts. 2013

[12] Yoganandan, N., Chirvi, S., et al. Foot–ankle fractures and injury probability curves from post-mortem human surrogate tests. *Annals of biomedical engineering*, 2016. 44(10): p. 2937-2947

[13] Pintar, F.A., Schlick, M.B., et al. Biomechanical response of military booted and unbooted foot-ankle-tibia from vertical loading. 2016, SAE Technical Paper.

[14] Chirvi, S., Pintar, F., et al. Human Foot-Ankle injuries and associated risk curves from under body blast loading conditions. 2017, SAE Technical Paper.

[15] Hampton, C.E., Kleinberger, M., Schlick, M., Yoganandan, N., and Pintar, F.A. Analysis of force mitigation by boots in axial impacts using a lower leg finite element model. 2020, SAE Technical Paper.

[16] Funk, J.R., Crandall, J.R., et al. The axial injury tolerance of the human foot/ankle complex and the effect of Achilles tension. *J. Biomech. Eng.*, 2002. 124(6): p. 750-757

[17] Yoganandan, N., Pintar, F., Kumaresan, S., and Boynton, M. Axial impact biomechanics of the human foot-ankle complex. 1997

[18] Science, N. and Organization, T. A survey of blast injury across the full landscape of military science. 2011

[19] Guillemot, H., Besnault, B., et al. Pelvic injuries in side impact collisions: a field accident analysis and dynamic tests on isolated pelvic bones. *SAE transactions*, 1997: p. 3624-3633

[20] Bailey, A.M., Christopher, J.J., Brozoski, F., and Salzar, R.S. Post mortem human surrogate injury response of the pelvis and lower extremities to simulated underbody blast. *Annals of biomedical engineering*, 2015. 43(8): p. 1907-1917

[21] Gayzik, F.S., Moreno, D.P., Vavalle, N.A., Rhyne, A.C., and Stitzel, J.D. Development of a full human body finite element model for blunt injury prediction utilizing a multi-modality medical imaging protocol. *Proceedings of 12th International LS-DYNA User Conference, Dearborn, MI*, 2012.

[22] Vavalle, N.A. Validation of the Global Human Body Models Consortium mid-sized male model in lateral impacts and sled tests. 2012, Wake Forest University.

[23] Funk, J.R., Tourret, L.J., George, S.E., and Crandall, J.R. The role of axial loading in malleolar fractures. *SAE transactions*, 2000: p. 212-223

[24] Rudd, R., Crandall, J., Millington, S., Hurwitz, S., and Höglund, N. Injury tolerance and response of the ankle joint in dynamic dorsiflexion. 2004, SAE Technical Paper.

[25] Siegler, S., Chen, J., and Schneck, C. The three-dimensional kinematics and flexibility characteristics of the human ankle and subtalar joints—Part I: Kinematics. 1988

[26] Kerrigan, J.R., Bhalla, K.S., et al. Experiments for establishing pedestrian-impact lower limb injury criteria. 2003, SAE Technical Paper.

[27] Untaroiu, C., Darvish, K., Crandall, J., Deng, B., and Wang, J.-T. A finite element model of the lower limb for simulating pedestrian impacts. 2005, SAE Technical Paper.

[28] Salzar, R.S., Genovese, D., et al. Load path distribution within the pelvic structure under lateral loading. *International journal of crashworthiness*, 2009. 14(1): p. 99-110

[29] Gabler, L.F., Panzer, M.B., and Salzar, R.S. High-rate mechanical properties of human heel pad for simulation of a blast loading condition. *Proceedings of Proceedings of the IRCOBI Conference*, 2014.

[30] Weaver, C., Guleyupoglu, B., Miller, A., Kleinberger, M., and Stitzel, J.D. Pelvic Response of a Total Human Body Finite Element Model During Simulated Injurious Under Body Blast Impacts. *ASCE-ASME J Risk and Uncert in Engrg Sys Part B Mech Engrg*, 2020

[31] Agreement, N.S. Protection Levels For Occupants Of Logistic And Light Armoured Vehicle. 2004, STANAG.

[32] Ott, K., Drewry, D., et al. Comparison of human surrogate responses in underbody blast loading conditions. *Journal of biomechanical engineering*, 2020. 142(9)

[33] Baker, W.A., Chowdhury, M.R., and Untaroiu, C.D. Validation of a booted finite element model of the WIAMan ATD lower limb in component and whole-body vertical loading impacts with an assessment of the boot influence model on response. *Traffic injury prevention*, 2018. 19(5): p. 549-554

[34] SAE, S. J211-1 instrumentation for impact test—Part 1—Electronic instrumentation. *SAE International*, 2007

VIII. Appendix

Figure A1 A and Figure A1 B show the pelvis and spine peak force response as a function of peak velocity (m/s) and time-to-peak (ms). Figure A1 C shows a boxplot of the peak forces for all body regions of interest for all 51 simulations (compilation of all peak velocities and time-to-peak ranges).

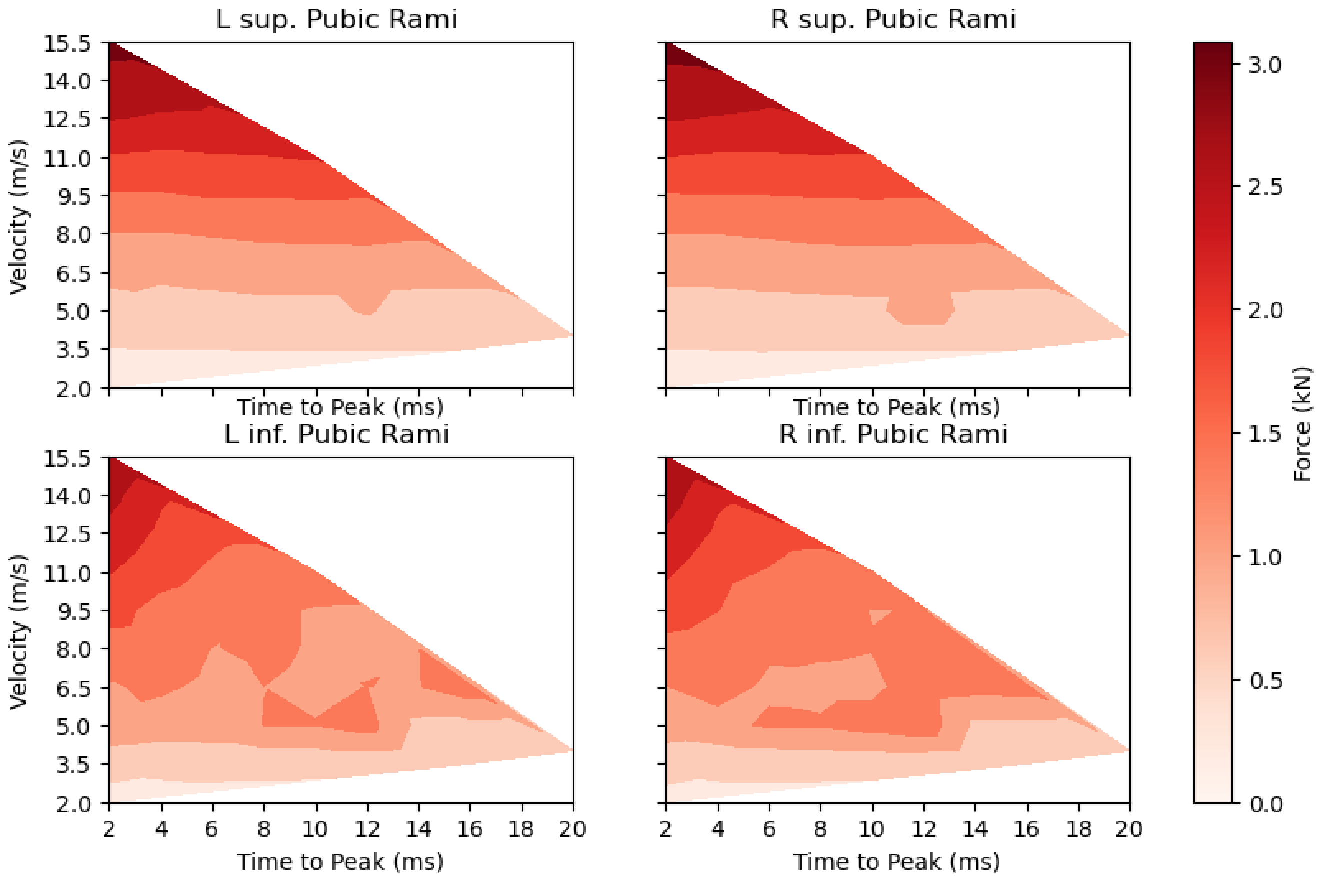

Figure A1 A. Peak force response for the superior and inferior pubic rami as a function of peak velocity (m/s) and time-to-peak (ms).

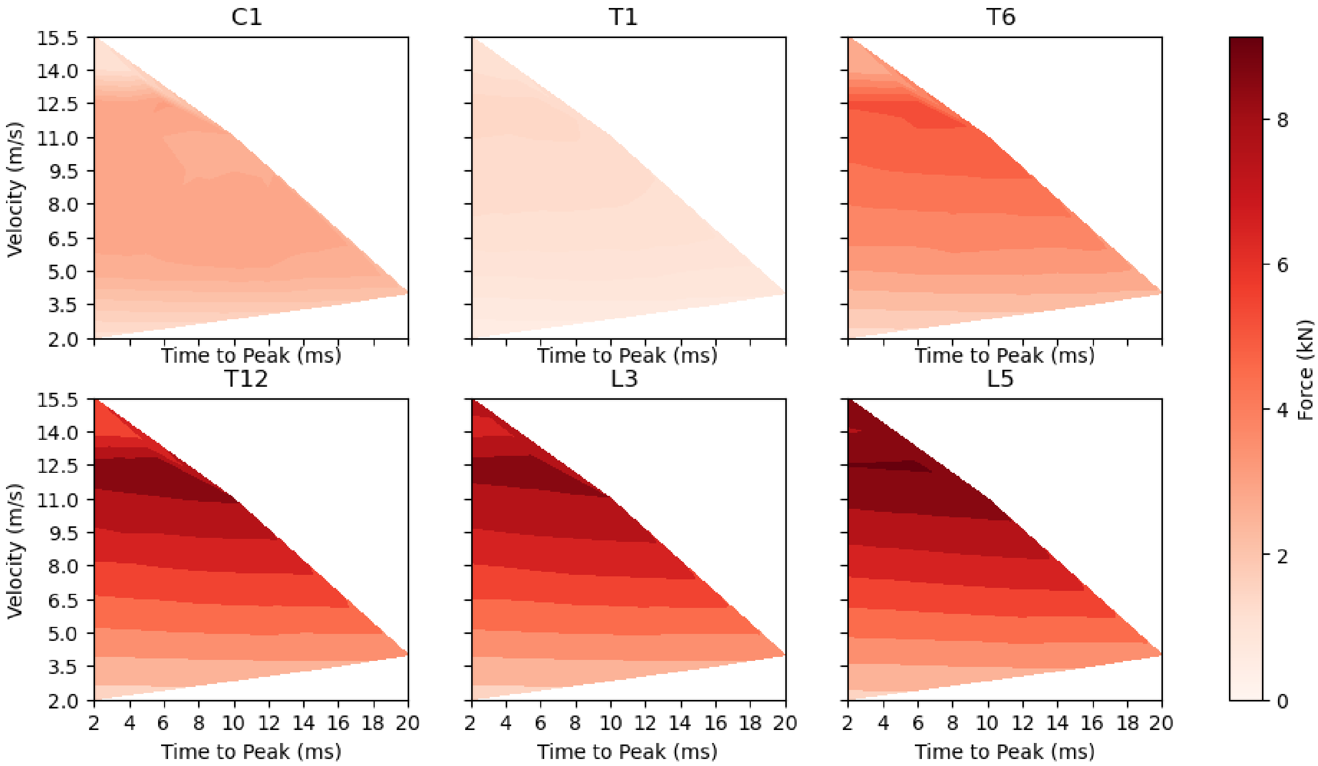

Figure A1 B. Peak force response for the spinal region as a function of peak velocity (m/s) and time-to-peak velocity (ms).

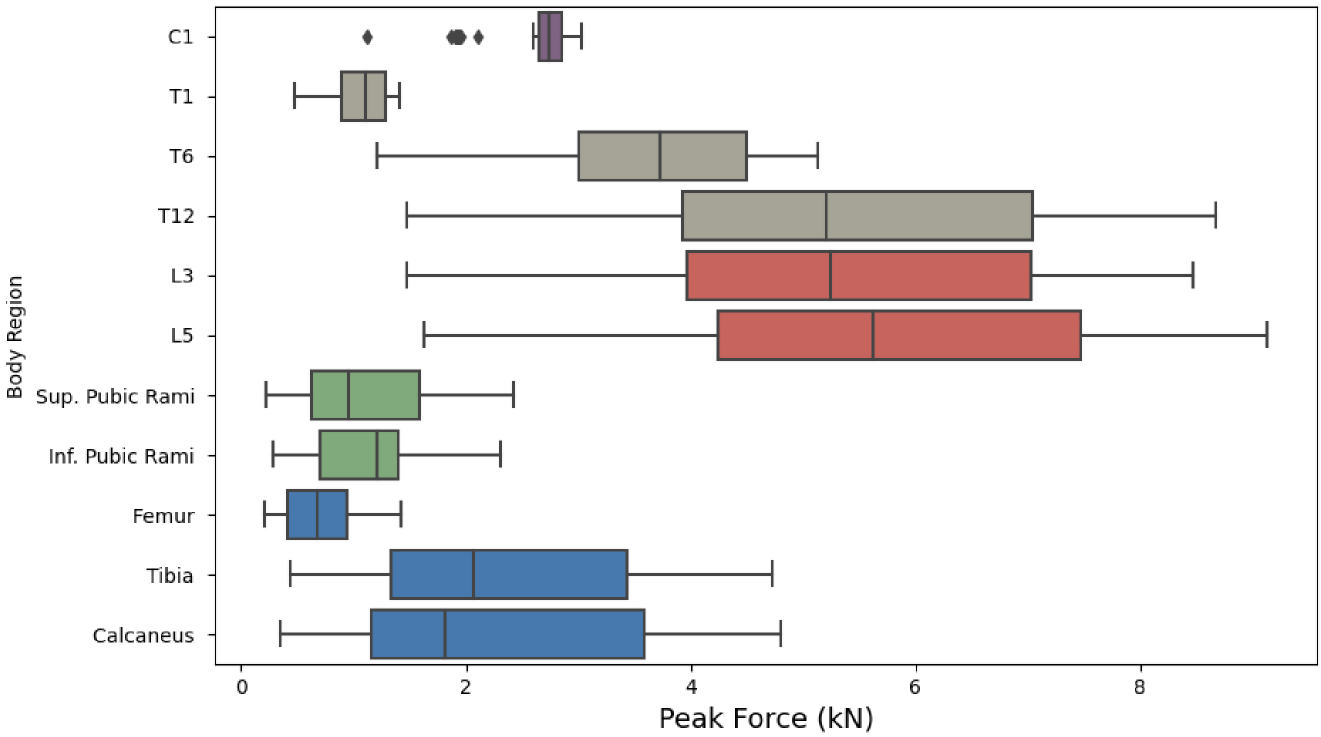

Figure A1 C. Box plots of peak force response for body regions of interest. The solid line represents the median value in the dataset